# Critical phenomena and phase structure of the perturbed Random Regular Graphs

Alexander Gorsky

Institute for Information Transmission Problems, Moscow

Landau Week, Erevan, June 24, 2023

Matrix model for massive spinless fermions on planar RRG
V.Kazakov, F. Levkovich-Maslyuk, V.Mishnyakov, A.G. , JHEP(2023)

Properties of RRG perturbed by short cycles(3 cycles - 6 cycles). Localization.
D.Kochergin, I.Khaymovich, O.Valba ,A.G arxiv;2305.14416

Phases of partially disordered RRG
O.Valba, A.G. Pisma v Zhetp (2022)
D.Kochergin, I. Khaymovich, O.Valba, A.G. In preparation

# Plan of the talk

- Motivation.
- Critical phenomena in RRG perturbed by chemical potentials for short cycles
- Matrix model for the massive spinless fermions on planar RRG. Derivation and critical behavior
- Phases in partially disordered RRG

# Two roles of RRG

- Discrete model of 2d quantum gravity. Can be considered in canonical ensemble with cosmological constant or in microcanonical ensemble - fixed area
- Model of Hilbert space for the interacting many-body system.
- Evidently perturbations of RRG in two frameworks have very different meaning

# The Perturbations of RRG

- Diagonal disorder- model for MBL phase
- Chemical potentials for number of short cycles. Number of nodes fixed.
- Massive fermionic determinant for the canonical ensemble--- chemical potentials for all number of nodes.
- Partially diagonal disordered RRG. Some nodes are clean
- General question - fragmentation of geometry induced by back reaction of matter

# Some facts on RRG

Number of graphs in ensemble
Large N

$$N_{RRG} = \frac{(dN-1)!!e^{-(d^2-1)/4}}{(d!)^N} = \\ = \frac{(dN)!e^{-(d^2-1)/4}}{2^{dN/2}(dN/2)!\,(d!)^N} \sim \left(\frac{eN}{d}\right)^{dN/2} .$$

Kesten-Mckay spectral density
Large N>>d

$$\rho_{KM}(\lambda) = \frac{d\sqrt{[4(d-1)-\lambda^2]}}{2\pi(d^2-\lambda^2)}$$

Isolated eigenvalues in the spectrum= clusters

Diameter of RRG

$$D_{RRG} \simeq \frac{2\ln N}{\ln(d-1)} , \quad d > 2 .$$

# General motivation. History

---RRG as model for the Hibert space. MBL toy model
Localization in the Hilbert space (Altshuler,Gefen,Kamenev,Levitov)
MBL — Basko,Aleiner,Altshuler + Gornyi,Polyakov,Mirlin
Localization on RRG( Mirlin,Fyodorov, Tarzia, Kravtsov,
Khaymovich, De Luca, Scardicchio,Tikhonov, Altshuler, Ioffe,
de Tomasi, Biroli,Ros, Zirnbauer, Lemarie,Roy.....

– Fragmentation of the RRG as a mechanism of localization
Turner,Mikhailidis, Abanin, Serbin,Huse,
. Moudgalya, Bernevig ,Regnault …..

– Quantum scars in the spectrum
Abanin, Serbin, Huse, Prosen, Pakourski, Klebanov....

– RRG and 2d quantum gravity interacting with matter.
Kazakov, Brezin, Migdal, Kostov, David, Mehta, Boulatov,
Parizi, Zinn-Justin,Zuber, Itzykson,Al.Zamolodchikov...

# RRG perturbed by k-cycles

Statistical model of exponential random graphs

$$Z(\mu_2, \mu_3 \ldots \mu_n) = \sum_{graphs} \exp(-\sum_{k}^{n} \mu_k Tr A^k)$$

We consider ensemble of random regular graphs . In terms of statistical mechanics it is mixed ensemble. Number of nodes is fixed while the chemical potentials, say, for 3-cycles and 4-cycles are introduced

# Clusterization transition in RRG

Avetisov,Hovhannesyan, Nechaev
Tamm,Valba A.G. 16'

$\mu > \mu_{crit}$

Clusterized phase

Chemical potential
for 3-cycles

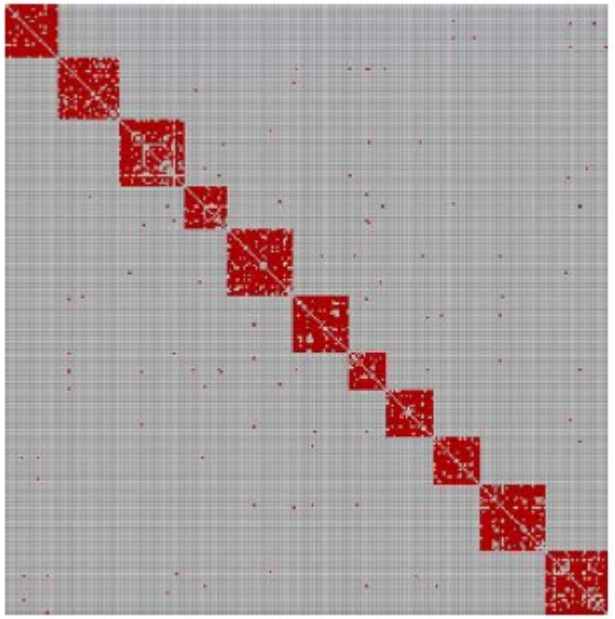

N/q clusters
for RRG

q - degree of node

The cluster sizes in RRG are the same. One-step replica symmetry breaking.

The clusters are the eigenvalue instantons in the spectrum.

# Spectral analysis of criticality.Eigenvalue instantons

Example of spectral density of adjacency matrix in the clusterized phase.d=20

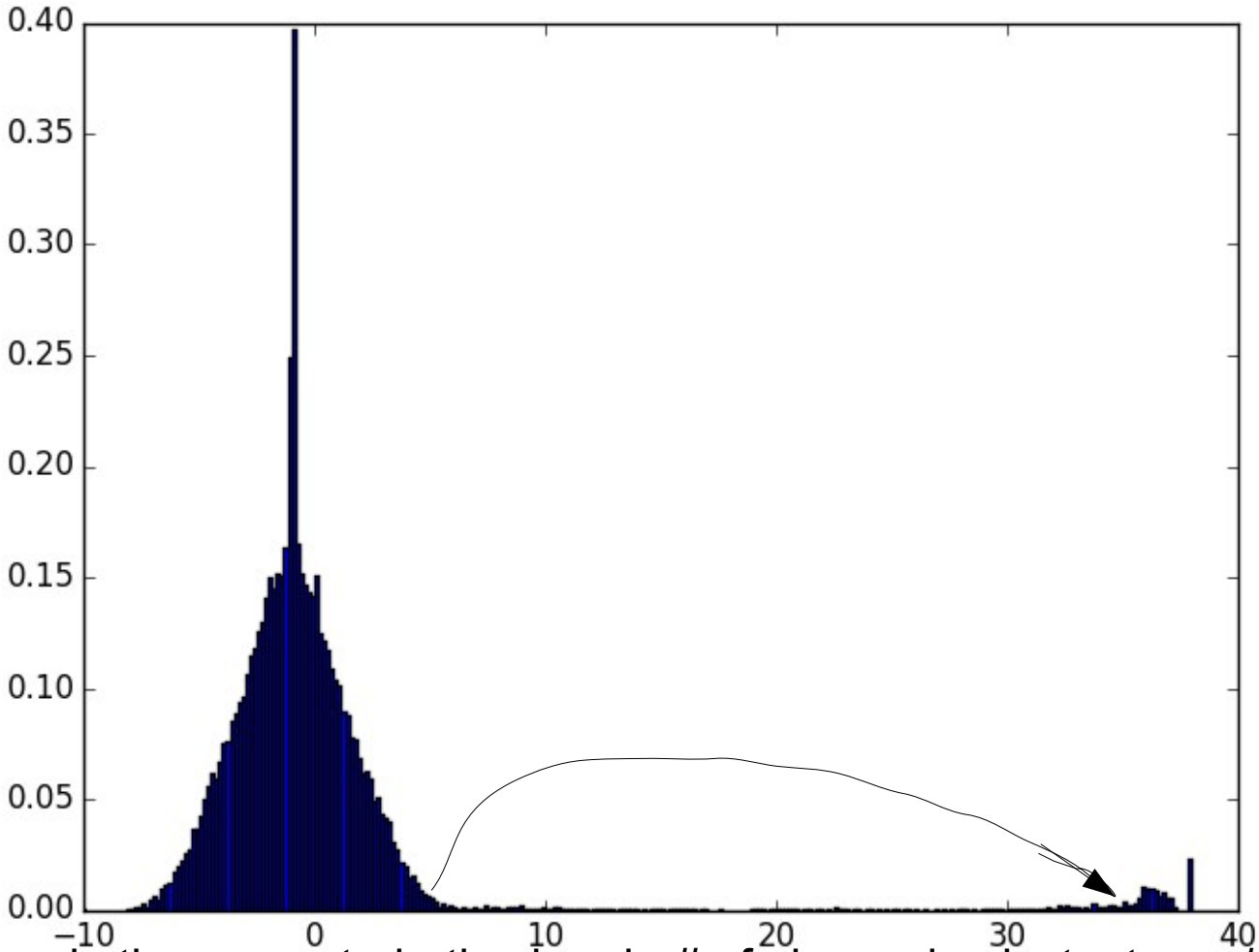


# of eigenvalues in the nonperturbative band =# of eigenvalue instantons=# clusters

Non-berturbative band - soft modes of the Laplacian

# RRG perturbed by 4-cycles and Thermofield double

$$Z(\mu_4) = \sum_{\{\text{states}\}}{}' e^{-\mu_4 N_4}$$

$\mu_4 > \mu_4^{cRRG}$

Above the critical value of the chemical potential
the RRG gets clusterized into bipartite clusters

Celly,Trugenberger,Biancolana 20'
Valba, A.G. 21'

If one more condition added bipartite clusters are of the special type - hypercubes
and correspond to a thermofield double state

The number of bipartite clusters is fixed by the node degree in RRG ensemble.

For all even k — the clusters are bipartite

# Phase structure and localization

Kochergin,Khaymovich. Valba, A.G.  23'

4 phases

– Unclustered phase

– TEN enriched phase --  precursor of clusterization

– Ideal cluster phase

--Phase of interacting clusters

We have analyzed numerically k=3-6 cycles

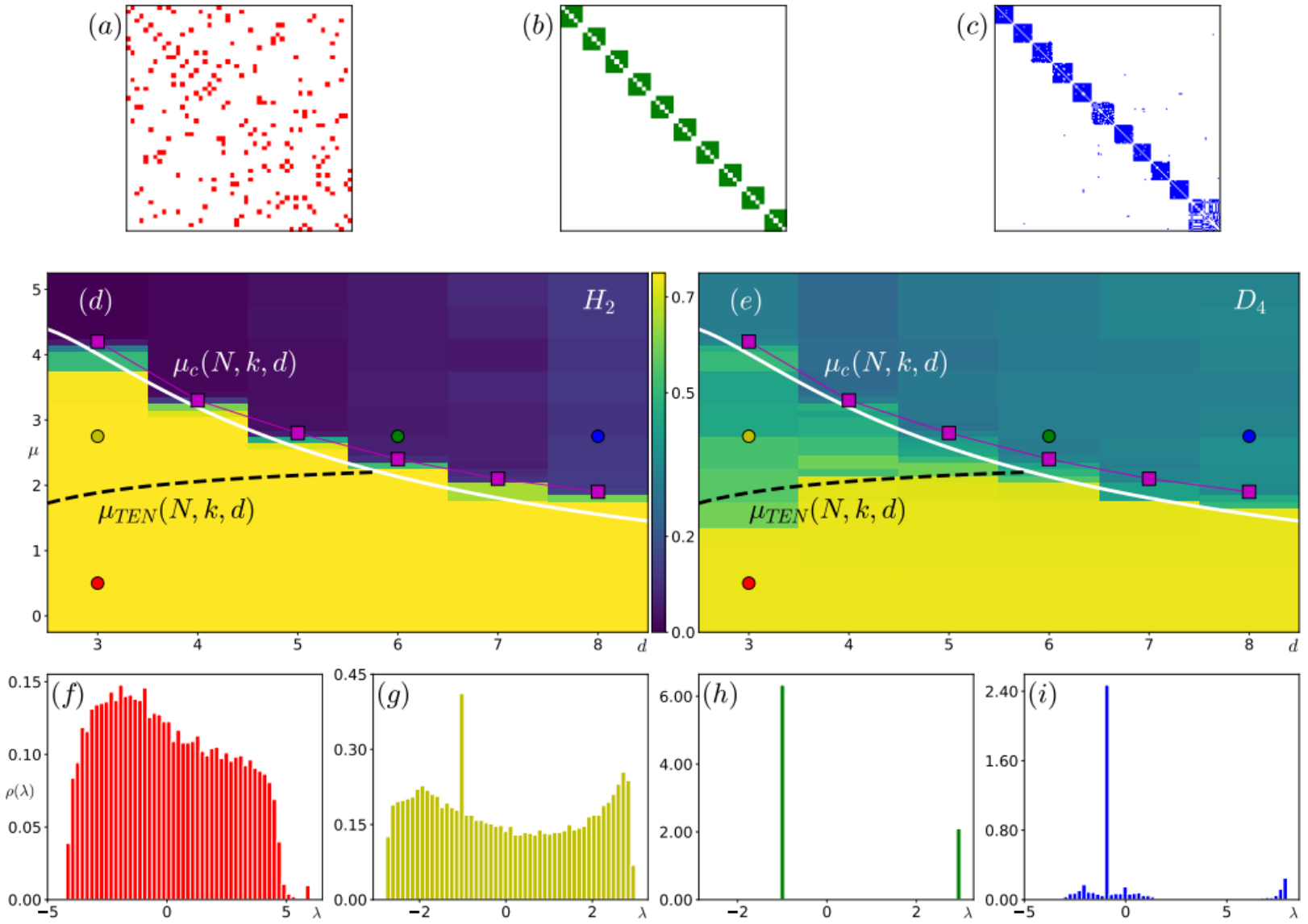


FIG. 1: Phase diagram in the plane "chemical potential – vertex degree" $(\mu_k, d)$ for finite-size RRG graphs for $N = 256$ and $k = 3$-cycles. (a-c) The cluster structure of RRG in (a) unclustered; (b) ideally clustered, and (c) interacting clustered phases. (d-e) Phase diagram, with drastic changes (d) in the density of states (DOS) via the Hellinger distance with respect to the ideal cluster, showing the clusterization transition (purple squares), and (e) in the higher-order fractal dimension $D_4$, sensitive to the scar states, given by the topologically equivalent nodes (TEN). Panels (f-i) show the averaged DOS in each of the 4 phases: (f) unclustered, (g) TEN-scarred unclustered, (h) ideally clustered, and (i) interacting clustered phases. The colors of the solid circles in the panels (d, e), marking each of 4 phases, correspond to the colors of the blocks in (a-c) and the DOS in (f-i). Solid white $\mu_c(N, k, d)$, Eq. (26), and dashed black $\mu_{TEN}(N, k, d)$, Eq. (34), lines show analytical estimates for the transition lines between

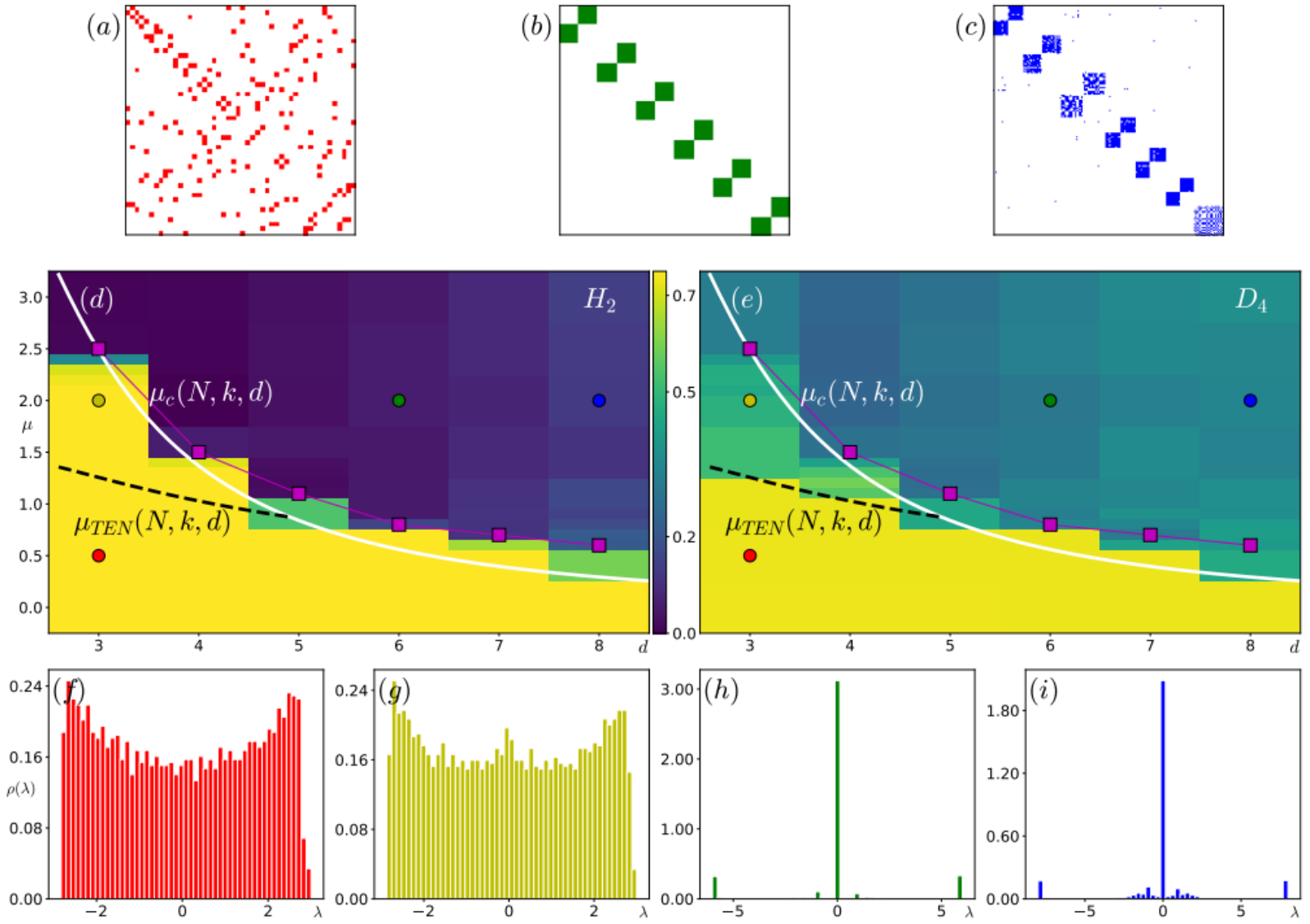


FIG. 10: Phase diagram in the plane "chemical potential – vertex degree" $(\mu_k, d)$ for finite-size RRG graphs for $N = 256$ and $k = 4$-cycles, similar to Fig. 1. (a-c) The cluster structure of RRG in (a) unclustered; (b) ideally lustered, and (c) interacting clustered phases. In the case of even $k$ the graph is bipartite in the clustered phase. -e) Phase diagram, with drastic changes (d) in the density of states (DOS) via the Hellinger distance with respect the ideal cluster, showing the clustering transition (purple squares), and (e) in the higher-order fractal dimension $D_4$, sensitive to the scar states, given by the topologically equivalent nodes (TEN). Panels (f-i) show the averaged OS in each of the 4 phases: (f) unclustered, (g) TEN-scarred unclustered, (h) ideally clustered, and (i) interacting clustered phases. The colors of the solid circles in the panels (d, e), marking each of 4 phases, correspond to the lors of the blocks in (a-c) and the DOS in (f-i). Solid white $\mu_c(N,k,d)$, Eq. (26), and dashed black $\mu_{TEN}(N,k,d)$, Eq. (34), lines show analytical estimates for the transition lines between the above phases.

# Phase structure. Critical lines

$$\mu_c(N,k,d) \simeq k\frac{(d-2)\ln N + 2\ln M - d\ln(d/e)}{d(d-1)^{[k/2]}} ,$$

Clusterization transition

$$M = \begin{cases} (d+1)\cdot[2\pi(d+1)]^{\frac{1}{2(d+1)}} , & k=3 \\ d\cdot[2\pi d]^{\frac{1}{2d}} , & k=4 \end{cases} .$$

$$\mu_{TEN,3} = \frac{1}{d-1}\left[(d-2)\ln N + d - \ln\sqrt{\pi d/2} - P(d)\right]$$

TEN saturation transition

$$P(d) \simeq 4(d-2)$$ ← Numerics

# Quantum scars in perturbative band

Kochergin,Khaymovich,Valba,AG 2023

Scar localized states.Localization occurs on specific subgraphs
Topologically equivalent nodes — TEN in perturbative band

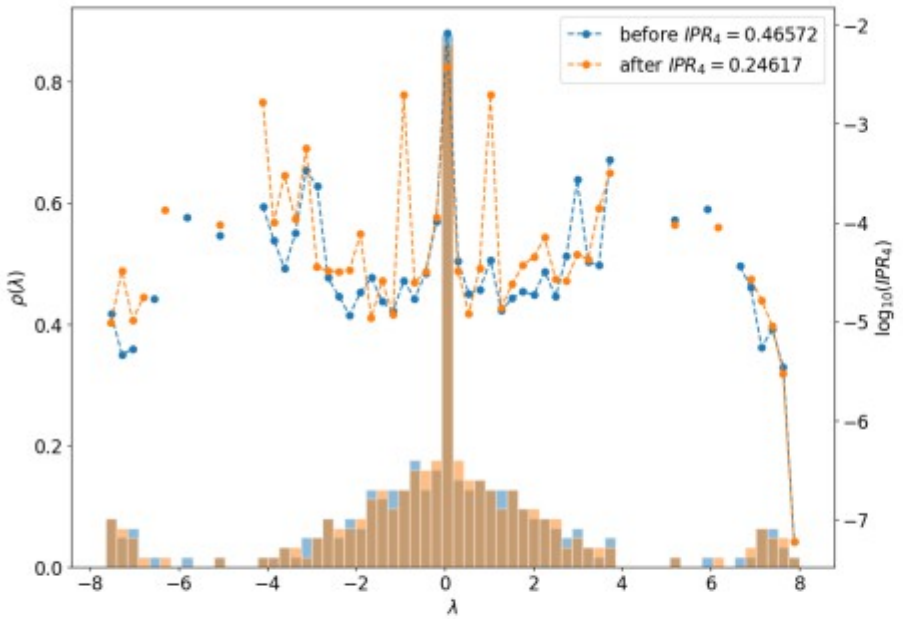


(a) Histograms show spectral densities, lines show $IPR_4$. State before (after) emergence of new local maxima of $IPR_4$ at $\lambda = \pm 1$ is marked by blue (orange) color

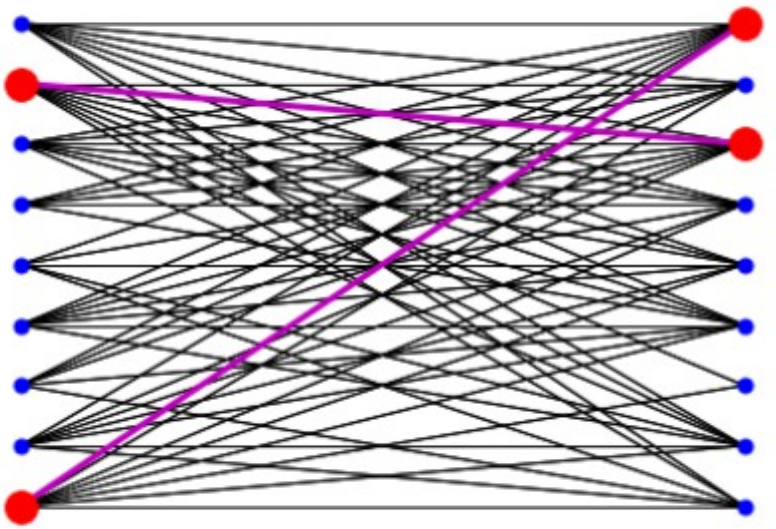

(b) TEN (red) with the nearest neighbors (blue). Edges that connected TEN are highlighted in magenta

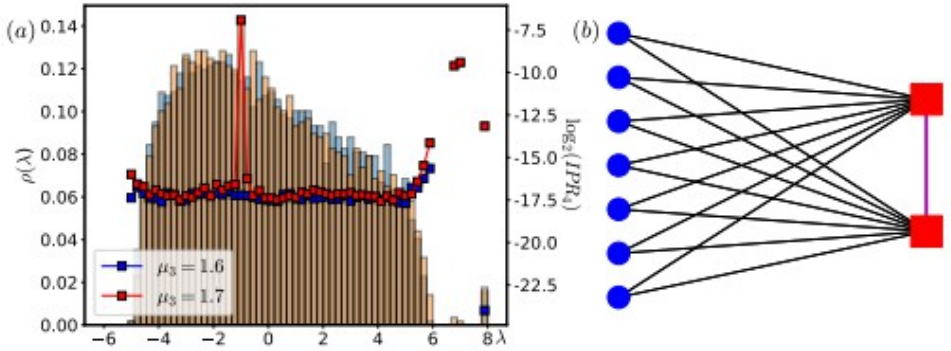


FIG. 4: (a) Evidence of TEN emergence in the density of states (color histograms) and energy-resolved $IPR_4$ (symbols) for $k = 3$-cycles. State before (after) jump discontinuity vs $\mu_k$ is marked by blue (orange) color. The amplitude of the local maximum at $\lambda = -1$ of both DOS and $IPR_4$ after the jump drastically increases. (b) Dipole TEN nodes (red squares) with the nearest neighbors (blue circles), that form a DOS peak at $\lambda = -1$. Edge, connecting TEN nodes is highlighted in magenta.

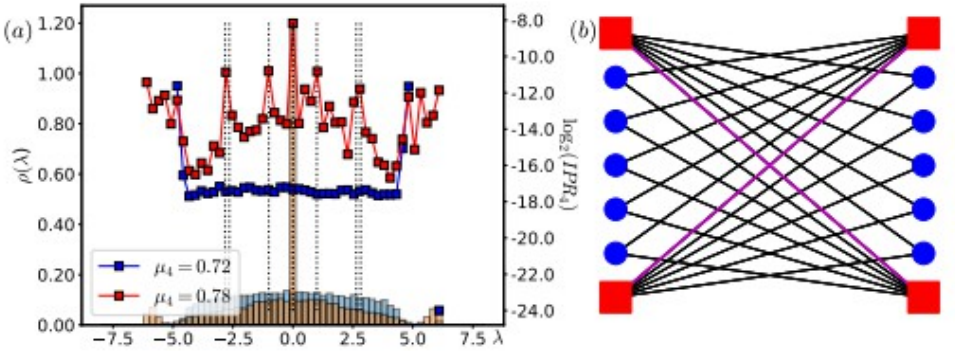


FIG. 6: (a) Evidence of additional TEN emergence at $\lambda = \pm 1, \pm\sqrt{7}, \pm\sqrt{8}$ (vertical dashed lines) in the density of states (color histograms) and energy-resolved $IPR_4$ (symbols) for $k = 4$-cycles. The notations are the same as in Fig. 4. (b) Two coupled TEN sets (red squares), with the nearest neighbors (blue circles), that form a DOS peak at $\lambda = \pm 1$. Edges, connecting TEN sets are highlighted in magenta.

Dipole and multipole interacting TENs

# Simplest scars at origin

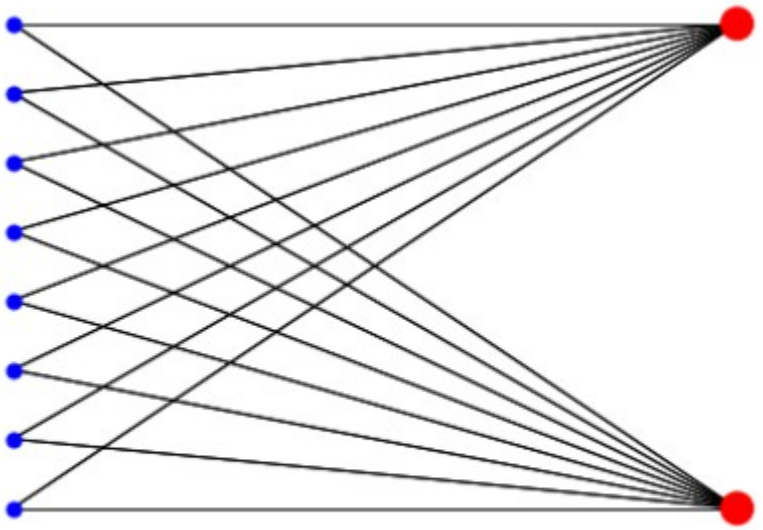

(b) TEN (red) with the nearest neighbors (blue)

Simplest dipole non-interacting TEN

# Remark.Scars from gravity viewpoint

Consider RRG as triangulation described by the adjacency matrix A.
TEN is equivalent to condition det A=0, the rank of the matrix A gets changed.

From the viewpoint of triangulation of surface change of the rank corresponds to the marked point on the surface — defect ( Fomin,Shapiro,Thornston 08)

Hence scars=TENs correspond to localization at the defect on the surface.

Some analogy with the gravitational scars localized near the black hole (Dodelson,Zhiboedov 22). Dual to the twist operators at the boundary

There was also attempt of holographic interpretation based on coadjoint Virasoro orbits  Liska, Gritsev et al 22'

# Surprise.Semi-Poisson in non-perturbative band

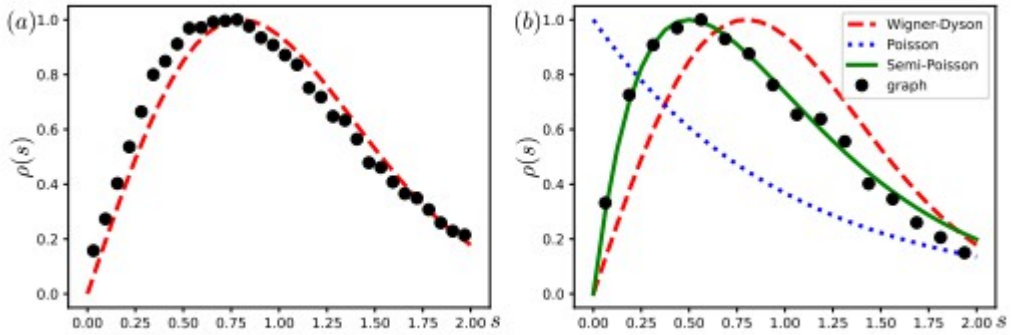


FIG. 7: Level spacing distribution for RRG in clustered phase for $k = 3$, $d = 20$, $N = 256$ separately for (a) the perturbative mid-spectrum band ignoring TEN states and (b) the non-perturbative side-band. Red dashed, blue dotted, and green solid lines show Wigner-Dyson ($\alpha = 1$, $\gamma = 0$), Poisson ($\alpha = 0$, $\gamma = 1$), and semi-Poisson ($\alpha = 1$, $\gamma = 1$) distributions, Eq. (55), respectively. Level spacing is calculated for the unfolded spectrum, Eq. (52), using 500 random realisations.

$$P(s) = C_1(\gamma, \alpha) s^{\alpha} e^{-C_2(\gamma,\alpha) s^{2-\gamma}}$$

# Localization at combined disorder:Structural+diagonal

Flat diagonal disorder W is added. The proceedure is as follows. First Identify the graph structure and then analyse the localization of states.

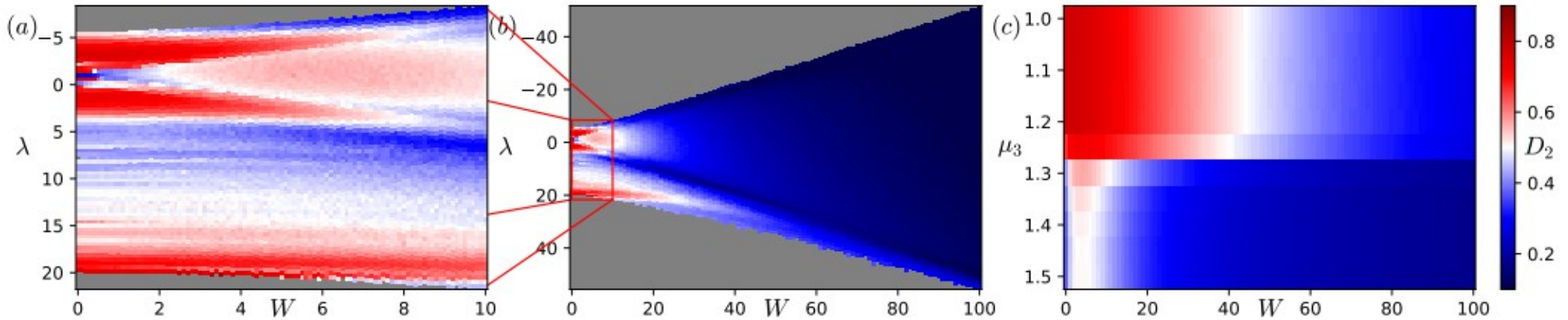


FIG. 9: The evolution of energy-resolved fractal dimension for RRG $N = 1024$, $d = 20$ in the interacting clusterized phase with diagonal disorder $W$, plotted versus (a, b) eigenenergies for $\mu_3 = 2$ for different $W$ ranges, as well as (c) the average fractal dimension versus the chemical potential $\mu_3$. Each point of a color plot is averaged over 20 (a, b) or 5 (c) structural and 5 (a, b, c) disorder realizations.

# Massive particle on planar RRG

Instead of the potentials V(L)~ Tr L^3 or Tr L^4 let consider the potential V(L, M^2) ~ Tr Log(L-M^2) = log det(L-M^2) which yields the power potentials for RRG ensemble discussed above as expansion at large mass M

Kazakov,Levkovich-Maslyuk,Mishnyakov, A.G , 22

$$Z = \sum_G \lambda^{|G|} \det[\mu \mathbb{I} - A(G)] = \sum_G \lambda^{|G|} \det[\frac{1}{2}\hat{M}^2 + \frac{1}{2}\Delta(G)]$$

The model has (at least) three different interpretations

--- 2d quantum gravity interacting with massive spinless fermions (q=3 node degree)

--- Statistical model of weighted rooted trees in a forest averaged over RRG ensemble

--- Hermitian one-matrix model with the non-trivial potential

# 2d gravity and matrix models.

- Consider the non-critical string . According to Polyakov we have to integrate over the worldsheet metrics which is taken into account via Liouville action

- Dimension of the target space D for string enters via power of determinant upon the integration over matter field.

- D=0 target space (c=0 theory) — no determinant

- D=-2 ,( c= -2 theory) — «fermionic determinant» positive power

--- Instead of the integration over the metrics — summation over the graphs Kazakov 85, David 85

– Summation over the graphs(RRG) gets substituted by the large N matrix model Whose perturbation theory reproduces the combinatorics of the summation over The graphs. Leading terms in N — planar graphs

# Partition functions

$$Z \equiv \log \zeta = \sum_{G} N^{2-2g} \lambda^{|G|} \det[m^2 + \Delta(G)]$$

--Sum is over random regular graphs (RRG) q=3

--pure gravity c=0 limit — no determinant at all

– c=-2 limit —massless determinant with zero mode removed

– finite mass- interpolation between two limits

$$Z(\Lambda_0, \eta, m_0) = \int Dg(\sigma) \int D\psi(\sigma) D\bar{\psi}(\sigma) \exp\Big[ - \int_{\mathcal{D}} d^2\sigma \sqrt{g} \left( g^{\alpha\beta} \partial_\alpha \bar{\psi} \partial_\beta \psi + m_0^2 \bar{\psi}\psi + \Lambda_0 + \kappa R \right) - \eta_0 \int_{\partial\mathcal{D}} ds \, [g(\sigma(s))]^{1/4} \Big] \qquad (1.1)$$

Continuum limit of partition function

# Matrix model for massive fermions coupled to 2d gravity. Derivation via Parisi-Sourlas trick

Let us use the Parisi-Sourlas trick applied for massless case by David and Kostov-Mehta. Reduce the dimension from D=0 to D=-2 by adding the anticommuting coordinates.

$$\zeta = \int D^{N^2}\Phi(\theta)\, e^{NS(\Phi)} = \int d^{N^2}\phi\, d^{2N^2}\psi\, d^{2N^2}\epsilon\, e^{NS(\Phi)}$$

$$\Phi(\theta) = \phi + \bar{\theta}\psi + \theta\bar{\psi} + \bar{\theta}\,\theta\epsilon$$

Action for superfield depending on mass and cosmological constant

$$S(\Phi) = \mathrm{tr}\int d^2\theta \left(-\frac{1}{2}\Phi^2(\theta) - \frac{1}{2}\partial_\theta\Phi(\theta)\partial_{\bar{\theta}}\Phi(\theta) + \frac{\lambda}{3}e^{-\frac{3}{2}M^2\bar{\theta}\theta}\left[\Phi(\theta)\right]^3\right)$$

# Potential for the matrix model

$$S(\Phi) = \mathrm{tr}\left[\frac{1}{2}\epsilon^2 - (\phi - \lambda\phi^2)\epsilon - \frac{1}{2}\lambda M^2\phi^3 + \bar{\psi}\psi - \lambda(\bar{\psi}\phi\psi + \bar{\psi}\psi\phi)\right].$$

$$\zeta = \int d^{N^2}\phi \, \det(1 - 2\lambda\phi) \; e^{N\mathrm{tr}\left[-\frac{1}{2}(\phi - \lambda\phi^2)^2 + \frac{1}{2}\lambda M^2\phi^3\right]}$$

$$X = \phi - \lambda\phi^2 \qquad *$$

Introduce the change of variables to cancel determinant

$$\zeta = \int d^{N^2}X \; e^{N\mathrm{tr}\left[-\frac{1}{2}X^2 + \frac{1}{2}\lambda M^2\phi^3(X)\right]}$$

We select only one root for the quadratic equation

$$S_X = \mathrm{tr}\left[-\frac{1}{2}X^2 + \frac{\lambda M^2}{2}\left(\frac{1-\sqrt{1-4\lambda X}}{2\lambda}\right)^3\right].$$

Shape of potential in the matrix model.
Two extrema and wall.

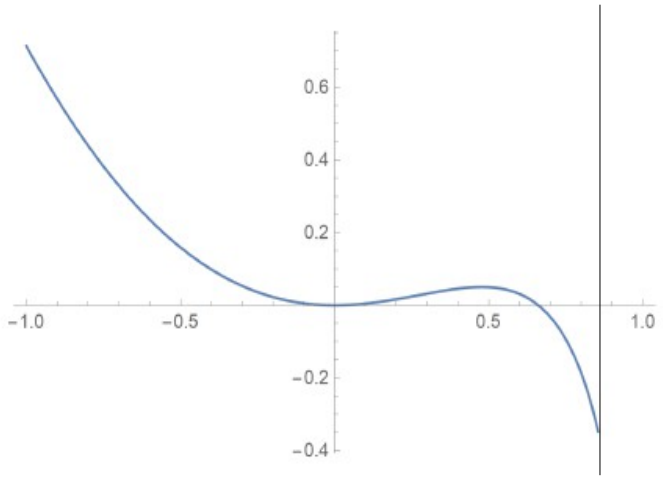


Figure 1: Potential for eigenvalue for $M = 1$ (without Vandermonde term). The eigenvalues should be confined in this well, below the branchpoint $x = 1/4$).

# Matrix model for massive fermions coupled to 2d gravity. Derivation via matrix-forest theorem

Matrix-tree theorem of Kirchoff  det' L =# (spanning trees) for any graph G where a zero-mode is removed at lhs

Generalization to the matrix-forest theorem  Chelnokov-Kelmans 74
David-Duplantier 88

All trees are rooted

$$\det[\frac{1}{2}\hat{M}^2 + \frac{1}{2}\Delta(G)] = \sum_{F=(F_1 \ldots F_l)\in G} \prod_{i=1}^{l} M^2 V(F_i) \qquad (3)$$

where $V(F_i)$ is the number of nodes in the tree $F_i$ and $M^2$ counts the number of trees in the forest.

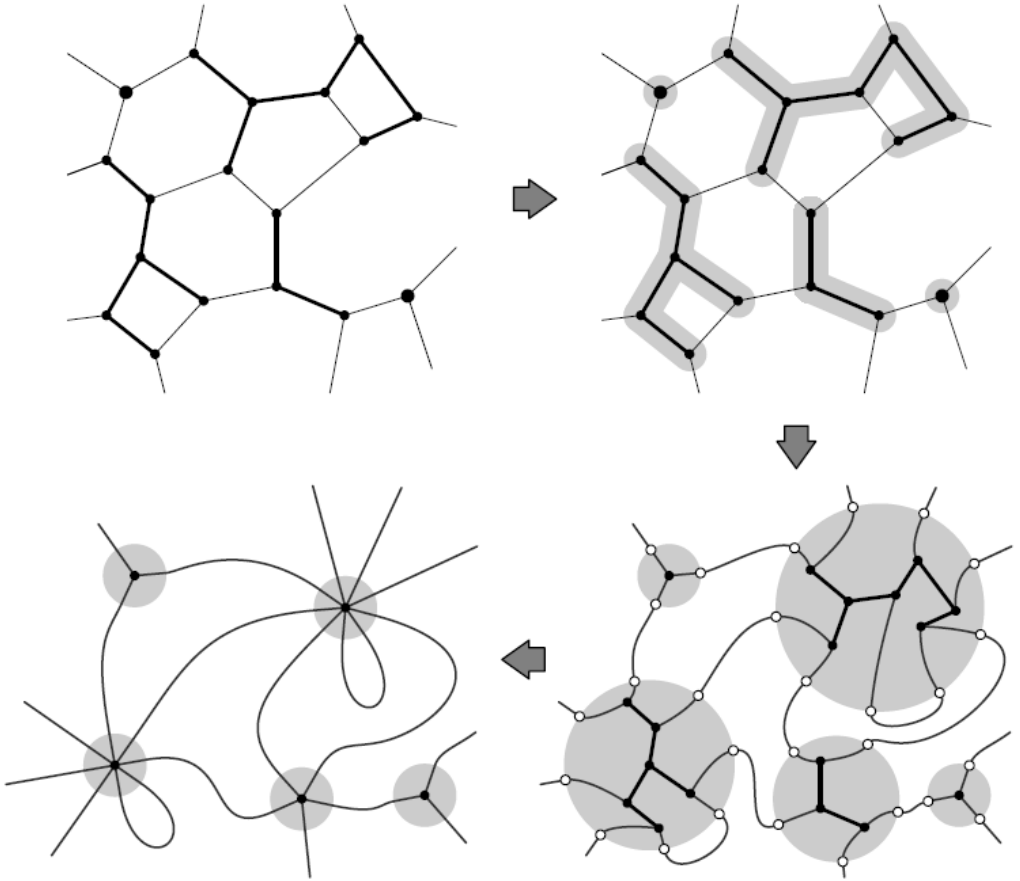

Step 1 — combinatorial brute force derivation of potential for the unrooted trees in a forest from matrix-forest theorem Bondesan, Caracciolo,Sportiello 17'

Step 2- derivation of the potential for the rooted trees in the forest

$$\tilde{V}(z) = \frac{1}{12z^2}\left(-6z^2 + (1-4z)^{3/2} + 6z - 1\right) = \sum_{n=1}^{\infty} \tilde{c}_n z^{n+2}, \qquad \text{where } \tilde{c}_n = \frac{(2n)!}{n!(n+2)!}.$$

$$\longrightarrow \frac{\lambda}{3}\left(\frac{1-\sqrt{1-4\lambda X}}{2\lambda}\right)^3 = \lambda\partial_\lambda\left(X^2\tilde{V}(\lambda X)\right)$$

# One-cut solution

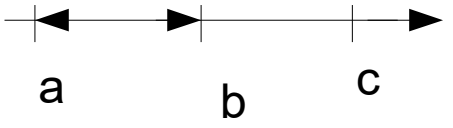


Resolvent

$$G(x)=\frac{1}{2}\left(x-\sqrt{(x-a)(x-b)}\right)$$
$$+\frac{9}{2}cM^2\left(1+\frac{2\left(a-\frac{2c}{3}\right)K}{\pi\sqrt{c}\sqrt{c-b}}\sqrt{\frac{x-b}{x-a}}-\frac{\left(x-\frac{2c}{3}\right)\vartheta_4'\left(\frac{\pi u}{2K}\right)}{\sqrt{c}\sqrt{x-c}\vartheta_4\left(\frac{\pi u}{2K}\right)}\right)$$

$\mathrm{sn}^2 u=\frac{x-c}{x-a}.$ Argument of elliptic K(m) $m=\frac{a-b}{c-b}$

$$B^2=c-b\ ,\ m=\frac{a-b}{c-b}$$

Equations providing the correct asymptotics of G(x)

$$\pi B^3(m-2)-18B^2\sqrt{c}M^2E+2\pi Bc\left(9M^2+1\right)-18c^{3/2}M^2K=0$$

$$3\pi B^4m^2-36B^3\sqrt{c}M^2((m-2)E-2(m-1)K)+108Bc^{3/2}M^2((m-2)K+2E)-48\pi=0$$

# Critical curve

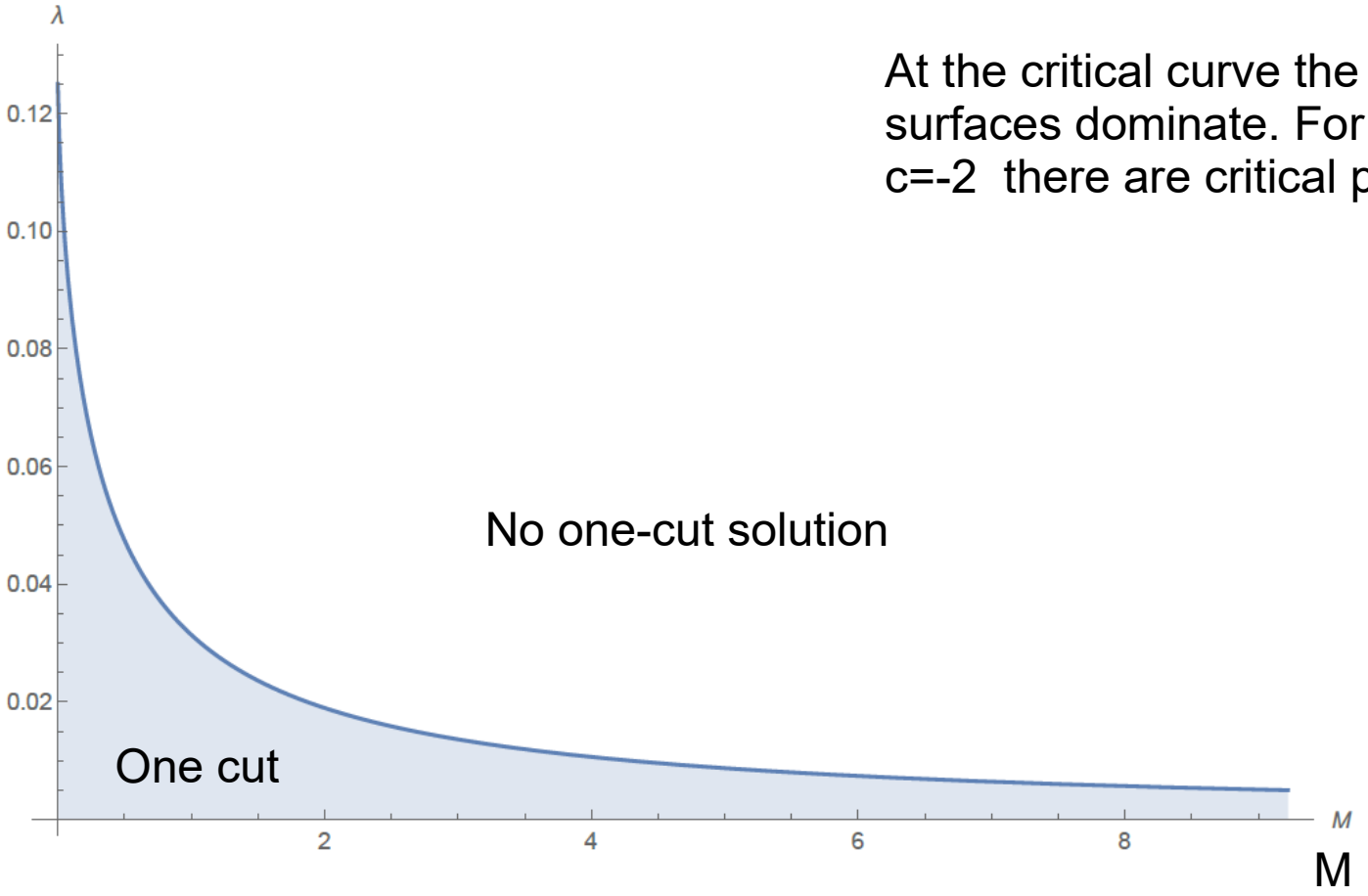


At the critical curve the large area surfaces dominate. For c=0 and c=-2 there are critical points

**Figure 3**. The critical curve $\lambda_c(M)$. The shaded area below the curve shows the allowed physical region on the $(M, \lambda)$ plane where the density is real and positive.

# Interpolation between three regimes

Large M limit. Pure gravity

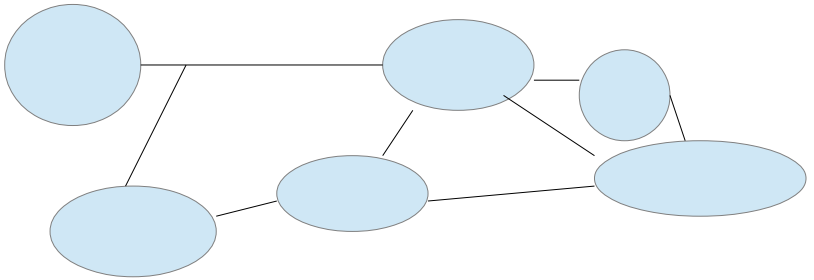

Finite intermediate M

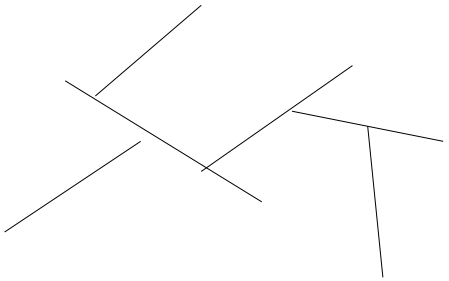

M=0 branched polymers phase

# Limit to pure 2d gravity

$M \to \infty$ Heavy fermions should decouple and pure gravity emerges

$M^2\lambda = \lambda_{eff}$ Effective cosmological constant is finite

$\lambda = \exp(-\beta_0)$ $\lambda_{eff}(M^2) = \exp(-\beta(M^2))$

Renormalization of cosmological constant by massive fermions

$\beta(M^2) = \beta_0 - \log M^2$

$(\lambda_{\mathrm{eff,crit}})^2 = \frac{1}{12\sqrt{3}}$ Critical value of the cosmological constant in pure gravity is reproduced correctly

# New double scaling limit

- Focus at the critical curve.
- Assume that there is new point M_c with new criticality. (M_c-M) L =const
- Perform the non-perturbative summation of all such terms
- Evaluate M derivative of the partition function=mean number of trees
- The number of fragments is finite!

# New double scaling. 2

$$z = \frac{p}{16M} = \text{finite}\ , \qquad M \sim p \to 0$$

Z-scaling variable, p~1/L

$$\Phi_s \sim 2\mathcal{J}(t^2 - 2t) + 3t^2 - 2t^3$$

This function counts the number
Of the components in the graph

Leading term in J

$$J = 512\pi^2 z - 72\sqrt{2}\pi \log(Mz) +$$
$$+ M\Big[ -81 \log^2(Mz) + 864\pi\sqrt{2} z \log(Mz) - 324(\sqrt{2}\pi - 1)\log(Mz)$$
$$-16384\pi^2 z^2 + 9216\pi(\pi - \sqrt{2})z\Big] .$$

$$\mathcal{J} = t - \log(m^2 t)$$

t- Lambert function

# Mobility edge in the partially disordered RRG

Valba, A.G. 22', D.Kochergin, I.Khaymovich, O.Valba, A.G in preparation

Consider the inhomogeneous Anderson model on RRG with « dirty» and « clean» nodes. The diagonal flat disorder at dirty nodes and no disorder at clean ones.

We study non-interacting spinless fermions hopping over RRG with connectivity $p = 3$ in a potential disorder described by Hamiltonian

$$H = \sum_{\langle i,j \rangle} \left( c_i^+ c_j + c_i c_j^+ \right) + \sum_{i=1}^{\beta N} \epsilon_i c_i^+ c_i, \tag{1}$$

where the first sum runs over the nearest-neighbor sites of the RRG, the second sum runs over $\beta N$ nodes with potential disorder. The energies $\epsilon_i$ are independent random variables sampled from a uniform distribution on $[-W/2, W/2]$. We consider gaps between adjacent levels, $\delta_i = E_{i+1} - E_i$, where the eigenvalues of a given realization of the Hamiltonian for a given total number of particles,

# Motivation for the model

- At many occations there are  topologically protected states in the many-body systems
- Zero modes strongly influence the localization and ergodicity properties
- Example. The topologically protected zero mode in IQHE is responsible for conductivity
- We mimic a zero mode sector in the physical space by the sector of «clean» nodes in the RRG. The ratio of numbers of clean and dirty nodes - parameter of the model

The delocalized strip gets formed from the clean nodes at arbitrary large disorder W.
The spectral density in the
central strip is well approximated by the Kesten-McKay with rescaled degree
Reason - solution of AAT eq at large W

$$d^* = (1-\beta)d$$

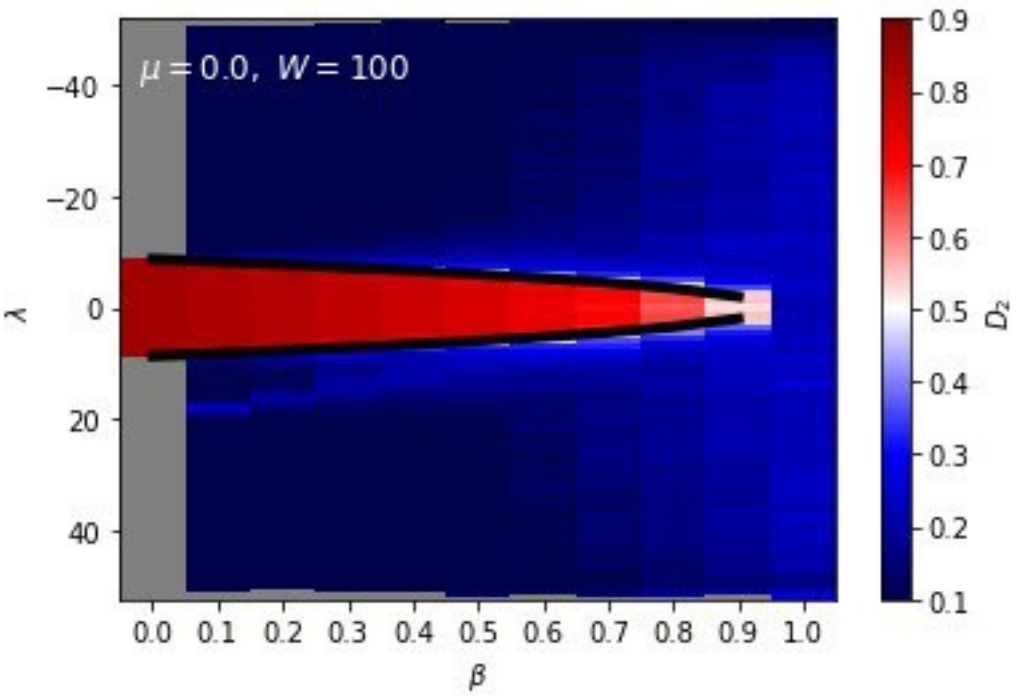


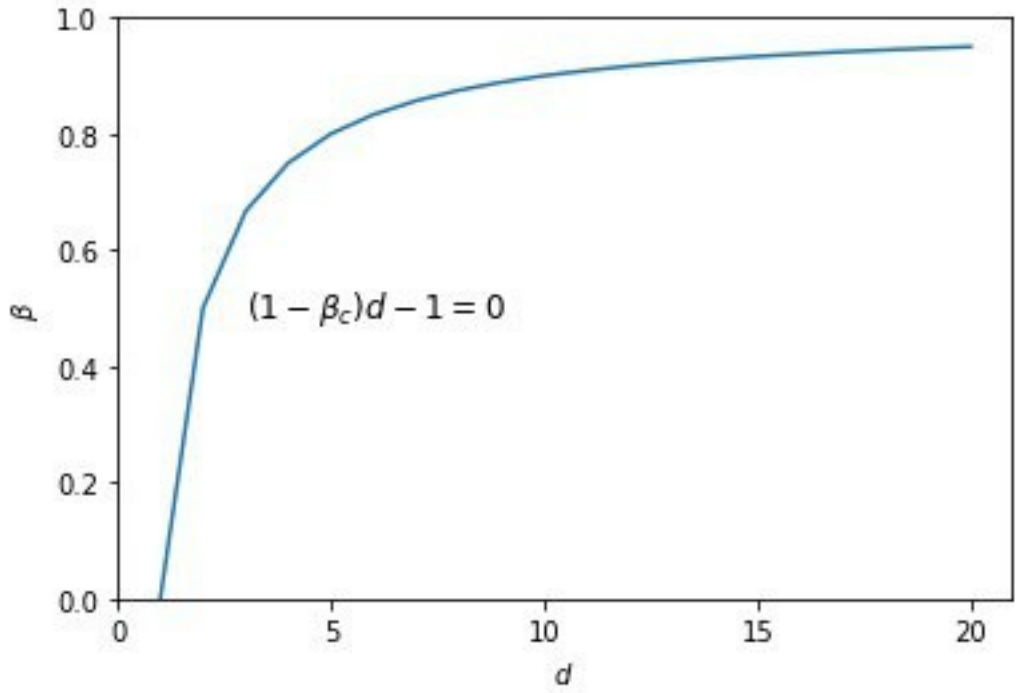


Critical curve separating the phases with delocalized strip and without the mobility edge.
Formula works well for sparse regime

# Interesting duality between sparse and dense phases

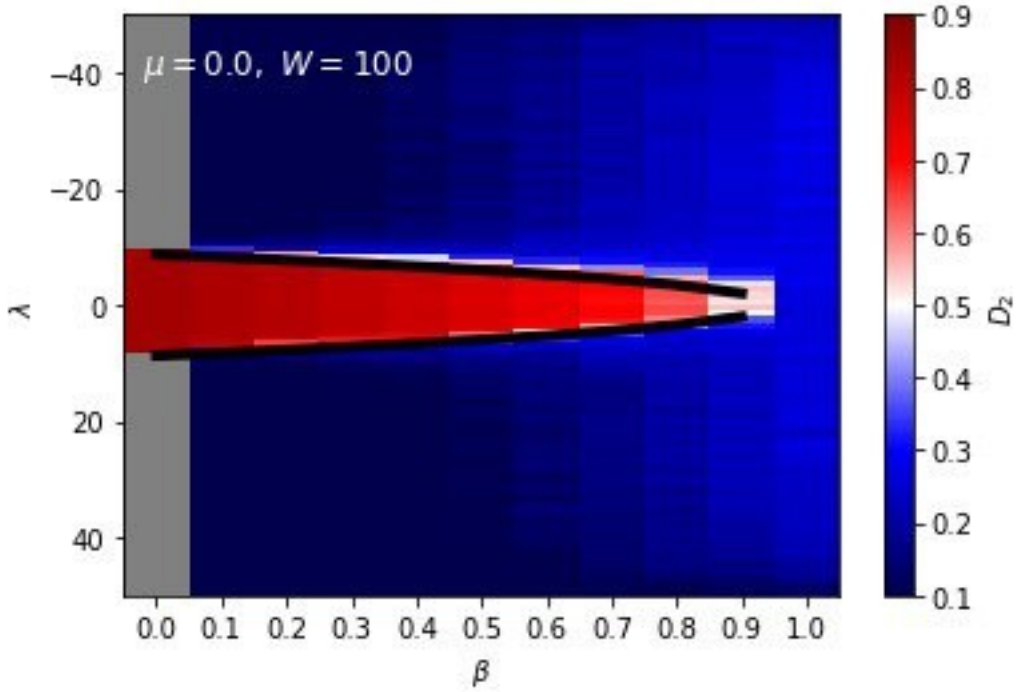


N=1024, d= 1004 The width of the delocalized band. Corresponds to d=20 - degree for complementary graph

# Conclusion

- Rich phase structure for k-cycle perturbed RRG. Surprises with localization.
- Due to the backreaction of matter the geometry effectively breaks down into fragments whose number depends on a fermion mass
- Matrix model provides the analytic answer for the fragmentation in the planar approximation
- 2d discrete gravity coupled to matter provides nontrivial insight for MBL
- Partially disordered RRG — mobility edge

Thanks for attention!

Stop the  war!